Compositional dependence of Raman frequencies in Si_xGe_{1-x} alloys*

Zheng Wenli(郑文礼)[1,2] and Li Tinghui(李廷会)[1,†]

[1]College of Electronic Engineering, Guangxi Normal University, Guilin 541004, China
[2]Department of Physics, Chengde Teacher's College for Nationalities, Chengde 067000, China

Abstract: Increases in Si content and the calculated Raman spectra acquired from the Si_xGe_{1-x} alloys reveal that the frequencies of the Ge–Si and Si–Si modes are up-shifted obviously, meanwhile that of the Ge–Ge optical mode is down-shifted, which is strongly dependent on their microstructural changes. The linear decrease and increase caused by their force constant (bond lengths and bond angles) changes, which can be used as a fingerprint to identify the average Si content. The complex microstructural changes induced by increasing Si content can be clearly displayed by Raman spectra transformation.

Key words: Raman spectroscopy; Si_xGe_{1-x} nanocrystals; DFT calculation
DOI: 10.1088/1674-4926/33/11/112001 **EEACC:** 2520

1. Introduction

Due to their adjustable electronic properties, Si_xGe_{1-x} alloys show many potential applications in optoelectronic and microelectronic devices such as integrated circuits, low-power radio-frequency chips, heterojunction bipolar and high performance field-effect transistors, integrated charge sensors, waveguide-integrated photonic modulators, photo-detectors, and solar cells[1−6]. These applications strongly depend on the fabrication of high-quality Si_xGe_{1-x} alloy and clear identification of the inner microstructural changes. However, the inner structure of Si_xGe_{1-x} alloy is complicated and thus the origins of many properties have not been understood well. This has hampered the applications of the alloy materials. Raman scattering has proved to be a useful tool to identify the size and composition of Si_xGe_{1-x} alloy nanostructures including nanoparticles, nanoislands, and superlattice layers[7−15]. Many investigations disclose that their properties mainly depend on their special inner structures, especially for larger size nanostructures, therefore revealing their complex inner structure has become very important. As is well known, the optical phonon modes related with Ge–Ge, Ge–Si and Si–Si vibration can be adopted to identify the overall formation of Si_xGe_{1-x} alloy nanostructures. However, mode behaviors that depend on their inner microstructural changes have not yet been clearly displayed. Recently, some weak modes at 420–470 cm^{-1} have also been detected and arbitrarily attributed to the Si–Si mode, which increases the mystery surrounding the Si_xGe_{1-x} alloy inner structure and stimulates extensive research to clarify its microstructural changes[16].

In this work, density functional theory (DFT) calculations are adopted to simulate the inner microstructural transformation induced by increasing Si content. The calculated Raman spectra disclose that the frequencies of the Ge–Ge mode are down-shifted linearly; meanwhile the frequencies of the Ge–Si and Si–Si modes are up-shifted linearly. In addition, some weak peaks originating from the local Si cluster surrounded by complex Ge/Si environments are also observed. All calculated results imply that the inner structures of Si_xGe_{1-x} alloy are obviously changed by Si content increases, and their complex structures are responsible for their novel optical phonon modes behaviors. With increasing Si content, the transformation process of Si_xGe_{1-x} alloy inner structures are clearly displayed via their Raman spectra transformation, meanwhile many special Raman modes origins are also further clarified. This work improves our understanding on the optical phonon mode behaviors in Si_xGe_{1-x} alloys, which can be used as a fingerprint to identify the complex Si_xGe_{1-x} alloy inner structures.

2. The model and calculation method

In our calculation, a density functional theory (DFT) study is performed on several supercells with different Si contents using the CASTEP packages. We use a 64-atom cubic supercell of Ge crystal in the diamond structure and randomly replace Ge atoms by Si ones until the desired composition is achieved[18]. In this way, we obtain nearly perfect random distributions of Si and Ge atoms in the supercells. The probability of the occurrence of Ge–Ge, Ge–Si, and Si–Si bonds in the supercell is close to $(1-x)^2$, $2x(1-x)$, and x^2, respectively. Before calculating the Raman spectra, the geometric structures of all the supercells are optimized using the BFGS minimizer in the CASTEP package with default convergence tolerances: 2×10^{-5} eV for energy, 0.05 eV/Å for maximum force, and 0.002 Å for maximum displacement. In the CASTEP framework, the norm-conserving pseudo-potential method is chosen together with gradient correction and the PErdew–Burke–Ernzerhof potential function. The other parameters are as follows: the energy cutoff for the plane-wave basis set is 450 eV, k-points are generated according to the Monkhorst–Pack grid with separations of 0.05 $Å^{-1}$, and the energy tolerance for self-consistency is 2×10^{-6} eV/atom[19−22]. Afterwards, the optimized geometrical structure is employed to construct and diagonalize the Hessian matrix:

* Project supported by the National Natural Science Foundation of China (Nos. 10847004, 61264008).
† Corresponding author. Email: tinghuili@tom.com
Received 20 April 2012, revised manuscript received 29 May 2012

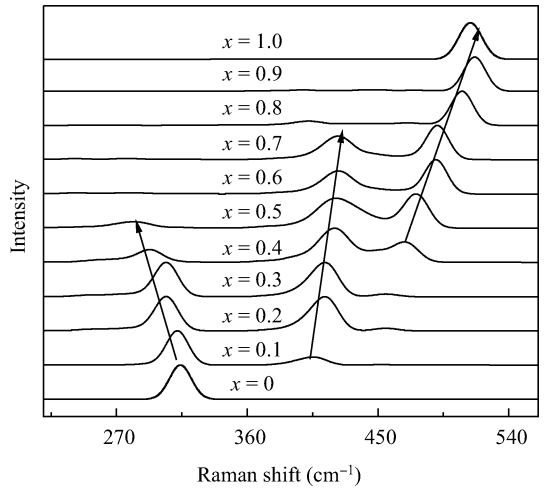

Fig. 1. The calculated Raman spectra of the Si_xGe_{1-x} alloy for Si content $x = 0$, 0.1, 0.2, 0.3, 0.4, 0.5, 0.6, 0.7, 0.8, 0.9 and 1.0.

$$D^{k,k'}_{\alpha,\alpha'} = \frac{1}{\sqrt{M_k M_{k'}}} \sum_{\alpha} \psi^{k,k'}_{\alpha,\alpha'} e^{-i\boldsymbol{q}\cdot\boldsymbol{r}_\alpha}, \quad (1)$$

where $\psi^{k,k'}_{\alpha,\alpha'}$ are the matrix force constants ($\alpha_{Si-Si} = 39.5$ N/m, $\alpha_{Ge-Ge} = 35.0$ N/m)[16]. The vibrational frequencies are obtained as the square roots of the phonon wavevector $\boldsymbol{q} = 0$. The ratio of atom mass and bond length of Si and Ge atoms are $m_{Si}/m_{Ge} = 0.39$, $r_{Si-Si}/r_{Ge-Ge} = 0.96$, respectively. The optimized supercell eigenfrequency can be simply written as[18]:

$$\omega_0^2 = 1/m_{Si(Ge)} \sum_{i=1}^{n} k_{GeSi(SiSi)}, \quad (2)$$

where $m_{Si(Ge)}$ is Si(Ge) atom mass and $k_{GeSi(SiSi)}$ are the corresponding parameters determined by the Ge–Si and Si–Si bond lengths and force constants. Those formulas indicate that its Raman mode behavior strongly depends on the composition change.

3. Results and discussion

The calculated Raman spectra acquired from the Si_xGe_{1-x} alloy with different Si contents are shown in Fig. 1 for comparison. It can be seen that a single-peak Raman spectra structure ($x = 0$) is replaced by double-peak feature ($x = 0.1$) due to Si atom addition. This can be explained as that a perfect Ge crystal only including the Ge–Ge mode is destroyed and some positions are occupied by Si atoms to form Ge–Si bonds, which causes a new mode dependent on the Ge–Si bond vibration to appear. In addition, a weak peak originating from Si–Si vibration is also observed for Si content at $x = 0.4$, which can be ascribed to the formation of some Si–Si bonds induced by the random distribution of Si atoms. So, three typical Raman peaks originating from Ge–Ge, Ge–Si, and Si–Si modes can be displayed clearly with increasing Si content. The Si content is increased from $x = 0.0$ to $x = 0.5$, the frequencies of the Ge–Ge mode are down-shifted from 314.3 to 283.3 cm^{-1} and its intensities are also decreased correspondingly. In this process, the prefect Ge crystal is destroyed and divided into some local Ge cluster surround by a Si/Ge atom. However, this physical mechanism is completely different from the Ge–Ge mode behavior in Ge nanocrystals. Previous research reveals that the frequencies of the Ge–Ge mode hardly depend on the nanoparticle size but can be obviously affected by an imposed stress effect[22]. The Si–Si bond length is smaller than that of the Ge–Ge bond, thus the added Si atoms will compress the local Ge cluster to affect its force constants. This process is equivalent to applying stress on the local Ge–Ge vibration thus pushing its frequencies to down-shift. With increasing Si content, the formed Ge–Ge bonds are slowly decreased and finally disappear at $x = 0.6$, meanwhile the numbers of Si–Si bond are synchronously increased. So the intensities of the Si–Si mode are also effectively enhanced. At $x = 0.7$, the decreasing Ge atoms also eliminate the Raman mode dependency of the Ge–Si bond. In this process, the frequency of the Ge–Si mode is up-shifted from 422.8 to 430.7 cm^{-1}, and that of the Si–Si mode is up-shifted from 469.2 to 520.4 cm^{-1}, which are also related with their microstructural changes. When the Ge atom number is lower than that of a Si atom, a local Si cluster will be formed and affected by surrounding Ge/Si atoms. From Eq. (2), we can find that the a large mass Ge atom replaced by a

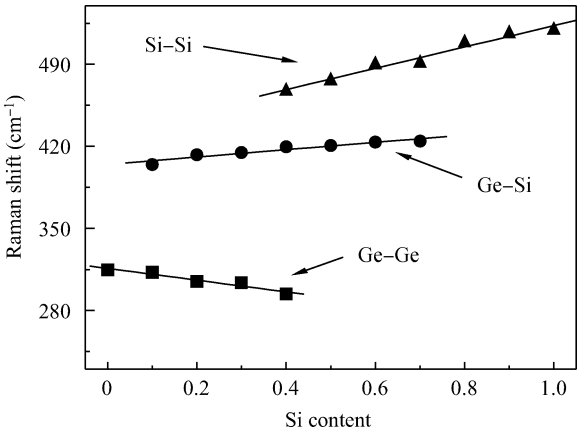

Fig. 2. The frequencies of Ge–Ge, Ge–Si and Si–Si modes as functions of Si content. The solid lines are fitting lines.

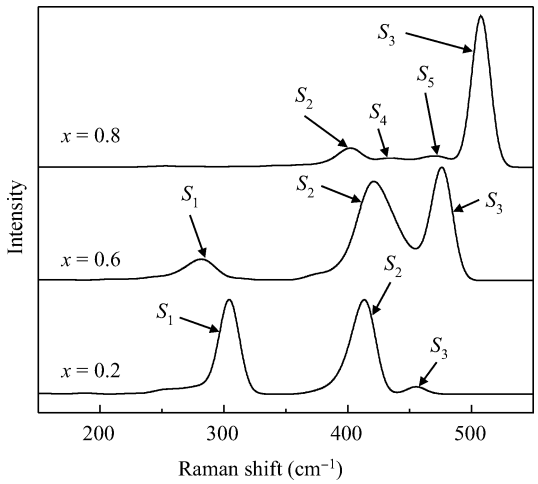

Fig. 3. The amplified Raman spectra of the Si_xGe_{1-x} alloys for Si content $x = 0.2$, 0.6 and 0.8.

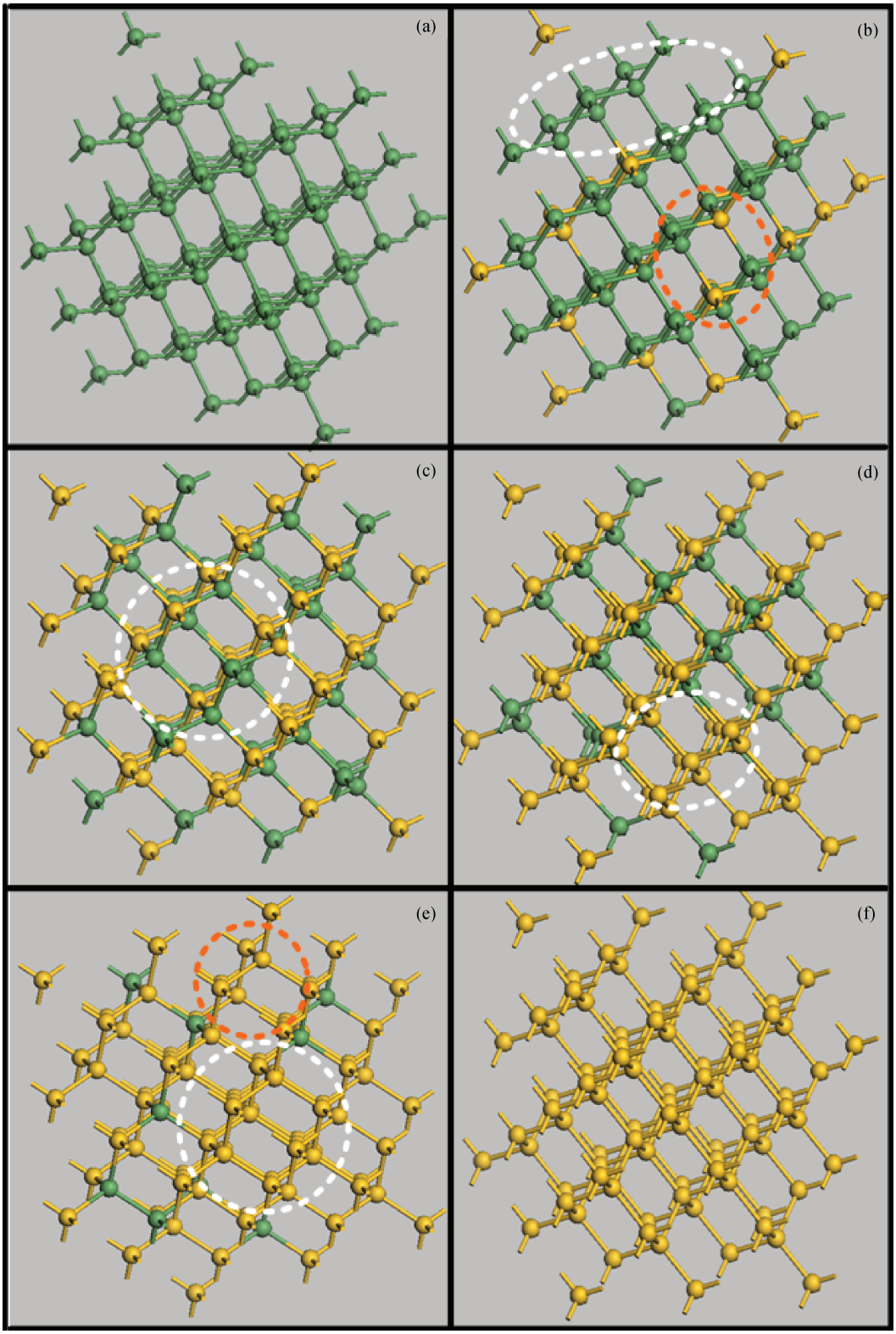

Fig. 4. (a)–(f) Schematic illustration of the Raman mode formation mechanism and microstructural transformation with increasing silicon content. Black and gray balls represent Ge and Si atoms, respectively.

small mass Si atom will effectively push the Si–Si optical mode up-shifts. The behaviors of the Ge–Si mode are similar to that of the Si–Si mode, because its origin is strongly dependent on the Si–Si mode.

To clearly display their mode behaviors, their frequencies of Ge–Ge, Ge–Si and Si–Si modes as functions of Si content are shown in Fig. 2. The Si–Si peak frequency increases linearly with composition changes, while the Si–Ge peak frequency also increases slowly over most of the composition range, which is in agreement with previous results[16]. On the contrary, the Ge–Ge peak frequency is decreased linearly. Therefore, the dependences of the Si–Si, Si–Ge and

Ge–Ge phonon frequencies on composition can be fitted linearly as[17]:

$$\omega_{\mathrm{Ge-Ge}}(x) = \omega_0^{\mathrm{Ge}} - \alpha x, \quad 0 < x < 0.45, \tag{3}$$

$$\omega_{\mathrm{Ge-Si}}(x) = \omega_0^{\mathrm{Ge-Si}} + \beta x, \quad 0.1 < x < 0.75, \tag{4}$$

$$\omega_{\mathrm{Si-Si}}(x) = \omega_0^{\mathrm{Si}} + \gamma(1-x), \quad 0.35 < x < 1.00, \tag{5}$$

where $\omega_0^{\mathrm{Ge}} = 309$ cm^{-1}, $\omega_0^{\mathrm{Ge-Si}} = 405$ cm^{-1}, and $\omega_0^{\mathrm{Si}} = 521$ cm^{-1} are the bulk Ge, $Ge_{0.5}Si_{0.5}$, and Si Raman frequencies, respectively, and the linear coefficients are found to be $\alpha = 50$ cm^{-1}, $\beta = 32$ cm^{-1}, and $\gamma = 91$ cm^{-1}. These simple linear behaviors can be used as a fingerprint to identify the composition changes in Si_xGe_{1-x} alloy.

Except for the three mode types of Ge–Ge, Ge–Si, and Si–Si, some weak peaks also appear in the calculated Raman spectra because of the complex inner structure in Si_xGe_{1-x} alloy, which is agreement with our previous experimental results[18]. The Raman spectra for $x = 0.2$, 0.6, and 0.8 are amplified and shown in Fig. 3. Except for the normal Ge–Ge (S_1) and Ge–Si (S_2) modes at $\sim$ 300 cm^{-1} and 400 cm^{-1} for Si content $x = 0.2$, a weak mode (S_3) at $\sim$ 454.9 cm^{-1} also appears, which can be ascribed to formed local Si–Si bond vibration. The size of the local Si–Si bond region is very small and affected strongly by surround Ge atoms, which can push its frequency down-shifts nearly to the Ge–Si mode. At $x = 0.6$, this mode (S_3) intensity is enhanced obviously and their frequency up-shifts accordingly, which is strongly related with the magnified local Si region. With further increasing Si content to $x = 0.8$, the Si–Si mode (S_3) frequency is further up-shifted and its intensity is further enhanced, which can be ascribed to a local larger sized Si cluster. Meanwhile, two weak peaks at $\sim$432.9 cm^{-1} (S_4) and 471.1 cm^{-1} (S_5) are also displayed, which are related with a local smaller size Si cluster. This result implies that the Si_xGe_{1-x} alloy inner is composed by a heterogeneous local Si cluster and surrounded by Ge atoms. It should be pointed out that only the Ge–Ge mode and the Si–Si mode exist in perfect Ge ($x = 0.0$) and Si ($x = 1.0$) crystals, as shown in Fig. 1. The detailed Raman spectra analysis discloses that complex structural transformations will occur inside Si_xGe_{1-x} alloy with increasing Si content, which can be clearly displayed by Raman spectra changes.

Figure 4 schematically illustrates the Si_xGe_{1-x} alloy inner structural transformation process when the Si concentration is increased. Firstly, a perfect Ge crystal without any Si atom is shown in Fig. 4(a) for comparison, only Ge–Ge modes can be observed in this structure. Secondly, added Si atoms divide the Ge crystal into a local Ge cluster (marked by white circle) surround by Si/Ge atoms [Fig. 4(b)], this structure pushes the Ge–Ge mode frequency down-shifts and the formed Ge–Si bonds (marked by black circle) are responsible for the Ge–Si mode origins. Thirdly, further increasing Si atoms will effectively decrease the local Ge clusters to form more Ge–Si bonds [Fig. 4(c)], which can enhance the Ge–Si mode intensity (marked by a white circle) and depress the Ge–Ge mode intensity. Fourthly, many Ge–Si bonds will be replaced by a Si–Si bond to form local Si clusters (marked by a white circle) [Fig. 4(d)] induced by continuously increasing Si atoms, which can cause Ge–Ge mode frequency up-shifts and intensity increases. Fifthly, superfluous Si atoms can not only form a large sized local Si cluster (marked by white circle) strongly dependent on the Si–Si mode (S_3) but also results in some small sized Si clusters (marked by a black circle) dependent on the two weak peaks (S_4 and S_5 in Fig. 3) [Fig. 4(e)], this structure becomes very complex. Finally, all Ge atoms are replaced by Si atoms and finally form a perfect Si crystal [Fig. 4(f)], which makes the complex alloy structure become simple and only the Si–Si mode appears. Based on analysis of the Raman spectra, this complex structural transformation process can be clearly displayed.

4. Conclusion

In summary, with increasing Si content, the calculated Raman spectra acquired from the Si_xGe_{1-x} alloy reveal that the Ge–Si and Si–Si optical modes are up-shifted obviously, meanwhile the Ge–Ge optical mode is down-shifted, which is strongly dependent on their microstructural changes. Their linear decreases and increases caused by the by the Si_xGe_{1-x} alloy inner structural changes (Ge and Si atom bond lengths, bond angles, and force constant) can be used as a fingerprint to identify the average Si content. In addition, some weak modes at $\sim$432.9 cm^{-1} (S_4) and 471.1 cm^{-1} (S_5) can also be observed, which are attributed to local Si clusters formed in the alloy inner. The complex microstructural changes induced by increasing Si content can be clearly displayed by the Raman spectra.

References

[1] Ross F M, Tromp R M, Reuter M C. Transition states between pyramids and domes during Ge/Si island growth. Science, 1999, 286: 1931

[2] Kuo Y H, Lee Y K, Ge Y S, et al. Strong quantum-confined stark effect in germanium quantum-well structures on silicon. Nature, 2005, 437: 1334

[3] Xiang J, Lu W, Hu Y J, et al. Ge/Si nanowire heterostructures as high-performance field-effect transistors. Nature, 2006, 441: 489

[4] Xiang J, Vidan A, Tinkham M, et al. Ge/Si nanowire mesoscopic josephson junctions. Nat Nanotechnol, 2006, 1: 208

[5] Liu L Z, Huang G S, Wang L L, et al. Ordered amorphous silicon nanoisland arrays and reflection spectral dependence on nanoisland geometrical parameters. Appl Phys Lett, 2009, 94:151903

[6] Liu L Z, Wu X L, Zhang Z Y, et al. Raman investigation of oxidation mechanism of silicon nanowires. Appl Phys Lett, 2009, 95: 093109

[7] Liu L Z, Wu X L, Li T H, et al. Twinning $Ge_{0.54}Si_{0.46}$ nanocrystal growth mechanism in amorphous SiO_2 films. Appl Phys Lett, 2010, 96: 173111

[8] Kolobov A, Oyanagi H, Usami N, et al. Raman scattering and X-ray absorption studies of Ge–Si nanocrystallization. Appl Phys Lett, 2002, 80: 488

[9] Cerdeira F, Pinczuk A, Bean J C, et al. Raman scattering from Ge_xSi_{1-x}/Si strainedlayer superlattices. Appl Phys Lett, 1984, 45: 1138

[10] Magidson V, Regelman D V, Beserman R, et al. Evidence of Si presence in self-assembled Ge islands deposited on a Si(001) substrate. Appl Phys Lett, 1998, 73: 1044

[11] Liu L Z, Wu X L, Gao F, et al. Size-independent low-frequency Raman scattering in Ge-nanocrystal-embedded SiO_2 films. Opt Lett, 2010, 35: 1022

[12] Ren S F, Cheng W, Yu P Y. Microscopic investigation of phonon modes in SiGe alloy nanocrystals. Phys Rev B, 2004, 69: 235327

[13] Qin L, Teo K L, Shen Z X, et al. Raman scattering of Ge/Si dot superlattices under hydrostatic press. Phys Rev B, 2001, 64: 075312
[14] Yndurain F. Vibrational properties of alloys: study of Si_xGe_{1-x}. Phys Rev B, 1978, 18: 2876
[15] Lannin J S. Vibrational and Raman-scattering properties of crystalline $Ge_{1-x}Si_x$ alloys. Phys Rev B, 1977, 16: 1510
[16] Alonso M I, Winer K. Raman spectra of c-$Si_{1-x}Ge_x$ alloys. Phys Rev B, 1989, 39: 10056
[17] Costa V R D, Tolle J, Powelit C D, et al. Compositional dependence of Raman frequencies in ternary $Ge_{1-x-y}Si_xSn_y$ alloys. Phys Rev B, 2007, 76: 035211
[18] Liu L Z, Wu X L, Shen J C, et al. Identification of local silicon cluster nanostructures inside Si_xGe_{1-x} alloy nanocrystals by Raman spectroscopy. Chem Commun, 2010, 46: 5539
[19] Liu L Z, Wu X L, Yang Y M, et al. Si–Si optical phonon behavior in localized Si clusters of Si_xGe_{1-x} alloy nanocrystals. Appl Phys A, 2011, 103: 361
[20] Pfrommer B G, Cote M, Louie S G, et al. Relaxation of crystals with the quasi-Newton method. J Comput Phys, 1997, 131: 233
[21] Hamann D R, Schluter M, Chiang C. Norm-conserving pseudopotentials. Phys Rev Lett, 1979, 43: 1494
[22] Perdew J P, Burke K, Ernzerhof M. Generalized gradient approximation made simple. Phys Rev Lett, 1996, 77: 3865
[23] Liu L Z, Gao F, Wu X L, et al. Influence of GeSi interfacial layer on Ge–Ge optical phonon mode in SiO_2 films embedded with Ge nanocrystals. Appl Phys Lett, 2009, 95: 171105